Monthly Notices
of the
ROYAL ASTRONOMICAL SOCIETY

MNRAS **431,** 3550–3556 (2013)
Advance Access publication 2013 April 9

doi:10.1093/mnras/stt439

The polarized gamma-ray burst GRB 061122

D. Götz,[1⋆] S. Covino,[2] A. Fernández-Soto,[3,4] P. Laurent[5] and Ž. Bošnjak[1,6]

[1]*AIM (UMR 7158 CEA/DSM-CNRS-Université Paris Diderot) Irfu/Service d'Astrophysique, Saclay, F-91191 Gif-sur-Yvette Cedex, France*
[2]*INAF – Osservatorio Astronomico di Brera, Via E. Bianchi 46, F-23807 Merate (LC), Italy*
[3]*Instituto de Fisica de Cantabria, CSIC-Universidad Cantabria, Avenida de los Castros s/n, E-39005 Santander, Spain*
[4]*Unidad Asociada Observatori Astronomic Universitat de Valencia – Instituto de Fisica de Cantabria, C/ Catedratico Jose Beltran 2, E-46980 Paterna, Spain*
[5]*APC (UMR 7164 CEA/DSM/Irfu, Université Paris Diderot, CNRS/IN2P3, Observatoire de Paris) 10, rue Alice Domon et Léonie Duquet, F-75205 Paris Cedex 13, France*
[6]*Department of Physics, University of Rijeka, HR-51 000 Rijeka, Croatia*

Accepted 2013 March 7. Received 2013 February 27; in original form 2013 February 1

ABSTRACT

We report on the polarization measure, obtained with IBIS on board *INTEGRAL*, of the prompt emission of GRB 061122. Over an 8 s interval containing the brightest part of the gamma-ray burst (GRB) we put a lower limit on its polarization fraction of 60 per cent at 68 per cent confidence level (c.l.) and of 33 per cent at 90 per cent c.l. on the 250–800 keV energy range.

We performed late time optical and near-infrared imaging observations of the GRB field using the Telescopio Nazionale Galileo and the Canada–France–Hawaii Telescope. Our multi-band (*ugrizYJHK*) photometry allowed us to identify the host galaxy of GRB 061122 and to build its spectral energy distribution. Using a photometric redshift code we fitted these data, and derived the basic properties of the galaxy, including its type and redshift, that we could constrain to the interval [0.57, 2.10] at a 90 per cent c.l., with a best-fitting value of $z = 1.33$.

The polarization measurement in different energy bands, together with the distance determination, allowed us to put the most stringent limit ($\xi \lesssim 3.4 \times 10^{-16}$) to date to a possible Lorentz invariance violation based on the vacuum birefringence effect, predicted by some quantum-gravity theories.

Key words: gravitation – polarization – gamma-ray burst: general – gamma-ray burst: individual: GRB 061122 – galaxies: photometry.

1 INTRODUCTION

Gamma-ray bursts (GRBs) are short-lived transients (ms to hundreds of seconds) of soft gamma-ray radiation that appear at random directions on the whole sky. Despite the recent progresses in the GRB field obtained mainly thanks to the *Swift* and *Fermi* satellites (see e.g. Gehrels, Ramirez-Ruiz & Fox 2009; Zhang et al. 2011), the nature of their prompt emission is still not clear. Nevertheless, thanks to the information obtained from their long-lived (hours to days) X-ray and optical counterparts, they have been proven to be of cosmological origin, with their redshifts, z, distributed in the range [0.1, ∼9], and some are firmly associated with Type Ib/c supernovae. These powerful explosions emit in a handful of seconds an amount of isotropic equivalent energy, $E_{\rm iso}$, that spans from 10^{50} to 10^{54} erg (e.g. Amati 2007), making them the most luminous events in the Universe, temporarily outshining all other sources. This huge amount of energy is nonetheless partially reduced, by accepting the hypothesis that GRBs are collimated sources (e.g. Rhoads 1997), and indeed the detection of some achromatic breaks in the light curves of GRB afterglows further supports the interpretation of GRBs as being produced in collimated jets, implying an energy reservoir of about 10^{51} erg (Frail et al. 2001; Bloom, Frail & Kulkarni 2003; Ghirlanda et al. 2012).

However, the precise content of this jet, and especially its magnetization, as well as the details of the mechanism leading to the gamma-ray emission are still not completely clear. Models range from unmagnetized fireballs, where the observed emission could be produced by relativistic ($\Gamma \gtrsim 100$) electrons accelerated in internal shocks propagating within the outflow (Rees & Mészáros 1994), to pure electromagnetic outflows where the radiated energy comes from magnetic dissipation (Lyutikov 2006). Intermediate cases with mildly magnetized outflows are of course possible (e.g. Spruit, Daigne & Drenkhahn 2001). Even in the case of an unmagnetized fireball, a local magnetic field in the emission region, generated by the shocks, is necessary if the dominant process is synchrotron radiation from relativistic electrons.

Recently, some measurements of polarization during the prompt emission of GRBs in the hundreds of keV energy range have been reported (Kalemci et al. 2007; McGlynn et al. 2007, 2009; Götz et al.

⋆E-mail: diego.gotz@cea.fr

2009; Yonetoku et al. 2011, 2012). These measurements can shed new light on the strength and scale of magnetic fields, as well as on the radiative mechanisms at work during the GRB prompt emission phase. Even if globally incoherent, in the case where the magnetic field is mainly transverse and locally highly ordered, i.e. has a local coherence scale which is larger than the typical size $\sim R/\Gamma$ of the visible part of the emitting region, the detected signal can still be highly polarized. On the other hand, in the case of a random field or an ordered magnetic field parallel to the expansion velocity, the polarization of the detected signal should vanish, except for the peculiar condition of a jet observed slightly off-axis (e.g. Lazzati et al. 2004).

Polarization measures in cosmological sources are also a powerful tool to constrain Lorentz Invariance Violation (LIV), arising from the phenomenon of vacuum birefringence as shown recently by Laurent et al. (2011a), Toma et al. (2012) and Fan, Wei & Xu (2007).

Here, we present the polarization results on the prompt emission of GRB 061122, obtained with the IBIS telescope on board *INTEGRAL* (Section 2), as well as the late time photometry of the GRB field observed with the Telescopio Nazionale Galileo (TNG) and the Canada–France–Hawaii Telescope (CFHT), that allowed us to identify the host galaxy and constrain its distance (Section 3). Finally (Section 4), we present the limits we could derive on the possible LIV predicted by some quantum gravity theories (like e.g. loop quantum gravity; see Gambini & Pullin 1999).

2 POLARIMETRIC RESULTS

2.1 *INTEGRAL* observations and data reduction

GRB 061122 has been detected by the *INTEGRAL* Burst Alert System (Mereghetti et al. 2003) on 2006 November 11, and localized to RA $= 20^{\rm h}15^{\rm m}20\overset{\rm s}{.}88$, Dec. $= +15^\circ30'50\overset{''}{.}8$, with a 90 per cent confidence level (c.l.) uncertainty of 2 arcmin (Mereghetti et al. 2006). With a peak flux of 31.7 ph cm^{-2} s^{-1} and a fluence of 2×10^{-5} erg cm^{-2} (20–200 keV) it ranks second among the GRBs detected by *INTEGRAL*, after GRB 041219A. It had a T_{90} duration of 12 s (Vianello, Götz & Mereghetti 2009), and a moderately high peak energy of about 160–170 keV (Golenetskii et al. 2006; McGlynn et al. 2009; Bošnjak et al. 2013).

IBIS (Ubertini et al. 2003) is a coded mask telescope on board the *INTEGRAL* satellite (Winkler et al. 2003). It is made by two pixellated detector layers, ISGRI (Lebrun et al. 2003) working in the 15 keV–1 MeV energy range and PICsIT (Di Cocco et al. 2003), working in the 200 keV–10 MeV energy range. The two layers are superposed and permit IBIS to be used as a Compton telescope by measuring the properties of the photons interacting in the two layers. Thanks to the polarization dependency of the differential cross-section for Compton scattering – linearly polarized photons scatter preferentially perpendicularly to the incident polarization vector – a Compton telescope can be used also as a polarimeter, and IBIS allowed us to detect polarization in three different objects, the Crab nebula (Forot et al. 2008), the black hole binary Cyg X–1 (Laurent et al. 2011b) and GRB 041219A (Götz et al. 2009). In this work, we adopt the same analysis technique as described in these references.

Due to the nature of Compton scattering, one can expect an azimuthal distribution of the scattered photons on the telescope lower plane of the form

$$N(\phi) = S[1 + a_0 \cos 2(\phi - \phi_0)], \quad (1)$$

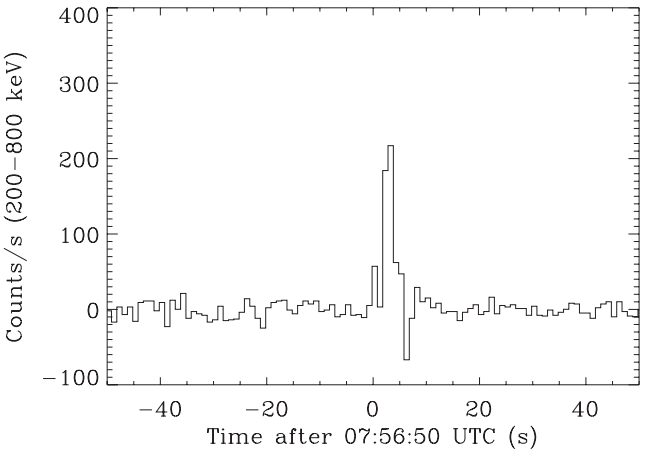

Figure 1. IBIS Compton events background-subtracted light curve of GRB 061122. The data gap towards the end of the GRB is due to telemetry transmission limitations at satellite level.

where PA $= \phi_0 - \pi/2 + n\pi$ is the polarization angle and $\Pi = a_0/a_{100}$ the polarization fraction, where a_{100} is the amplitude expected for a 100 per cent polarized source derived by Monte Carlo simulations of the instrument (see e.g. Forot et al. 2008).

To perform the polarization analysis, we derived the source flux as a function of ϕ, and the scattered photons were then divided in six bins of 30° as a function of the azimuthal scattering angle. To improve the signal-to-noise ratio in each bin, we took advantage of the π-symmetry of the differential cross-section, i.e. the first bin contains the photons with $0^\circ < \phi < 30^\circ$ and $180^\circ < \phi < 210^\circ$, etc. The chance coincidences (i.e. photons interacting in both detectors, but not related to a Compton event) have been subtracted from each detector image following the procedure described in Forot et al. (2008). The derived detector images were then deconvolved to obtain sky images, where the flux of the source in each bin is measured by fitting the instrumental point spread function to the source peak, building a so-called polarigram of the source.

2.2 Analysis and results

In Fig. 1, we report the IBIS background-subtracted light curve of GRB 061122, derived using the Compton events in the 200–800 keV energy range.

We performed the polarization analysis over different time intervals of the GRB. The best signal-to-noise ratio is obtained over the 07:56:50.0–07:56:58.0 UT time interval. In order to compute a_{100}, we derived the IBIS/ISGRI and SPI spectra over the same time interval with the technique developed by Bošnjak et al. (2013), and fitted them jointly with XSPEC v. 12.3.0 (Arnaud 1996). The data can be equally well fitted with a Band model (Band et al. 1993) or a power law with a high-energy cut-off. Since for the former the β parameter is not constrained we use the latter. The best-fitting photon index is $\alpha = -1.15 \pm 0.04$ and the cut-off energy $E_{\rm c} = 221 \pm 20$ keV (both errors are given at 90 per cent c.l.), corresponding to a peak energy of 188 keV, slightly higher than the one of the average spectrum. Given these spectral parameters, a_{100} has been computed through Monte Carlo simulations, and turns out to be independent of the energy band, being 0.29 ± 0.02 in the 250–800 keV energy band, 0.30 ± 0.03 in the 250–350 keV energy band and 0.29 ± 0.03 in the 350–800 keV energy band. We built the corresponding polarigrams in three energy bands (250–800, 250–350, 350–800 keV), and we fitted them with equation (1) using a least squares technique to

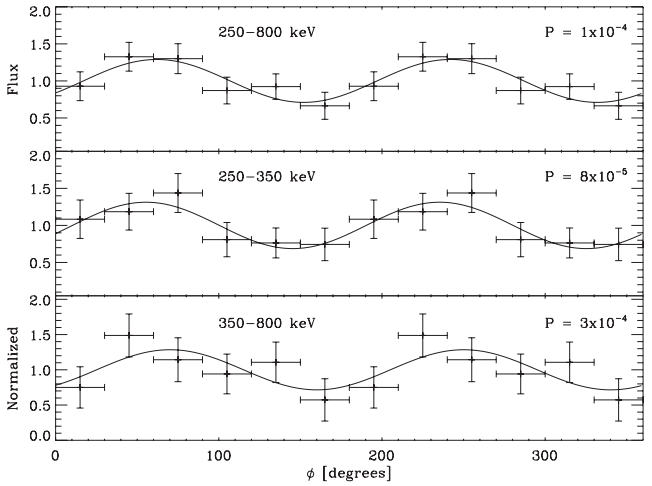

Figure 2. Polarigrams of GRB 061122 in different energy bands. The crosses represent the data points (replicated once for clarity) and the continuous line the fit done on the first six points using equation (1). The chance probability of a non-polarized (<1 per cent) signal is reported in each panel.

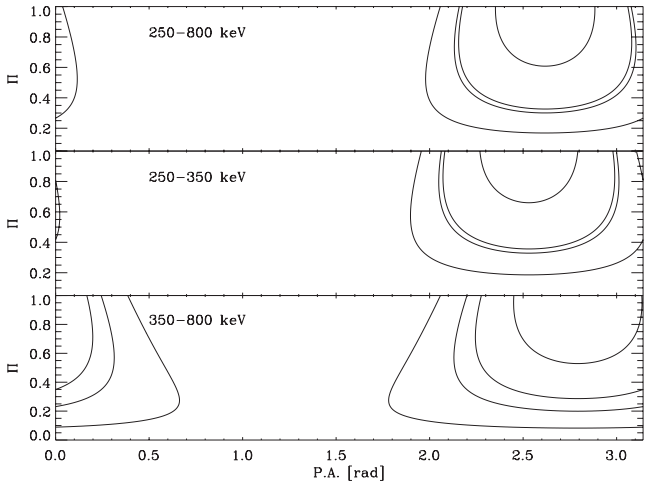

Figure 3. The 68, 90, 95 and 99 per cent (top to bottom in each panel) confidence contours for the Π and PA parameters for three energy ranges.

derive a_0 and ϕ_0, see Fig. 2. Confidence intervals on a_0 and ϕ_0 were, on the other hand, not derived from the fit, since the two variables are not independent. They were derived from the probability density distribution of measuring a and ϕ from N independent data points over a π period, based on Gaussian distributions for the orthogonal Stokes components (see equation 2 in Forot et al. 2008).

Over the selected time interval we measure a high polarization level in the 250–800 keV energy band, deriving a 68 per cent c.l. lower limit to the polarization fraction (Π) of 60 per cent and the polarization angle of 150 ± 15°. The corresponding polarigram is shown in the upper panel of Fig. 2. The 68, 90, 95 and 99 per cent confidence regions for the two parameters are shown in Fig. 3, where one can see that the 90 and 99 per cent c.l. lower limit to Π are 33 and 16 per cent, respectively. So despite the fact that the statistics is not high enough to fully constrain the polarization fraction, we can exclude that our signal is due to an unpolarized source (Π <1 per cent) at a probability level P of 10^{-4} (also shown in Fig. 2). The same analysis has been performed for the 250–350 and 350–800 keV energy bands, and the results are plotted in Figs 2 and 3, and reported in Table 1.

Table 1. Polarization measurements of GRB 061122.

Energy band (keV)	Π (per cent) (68 per cent c.l.)	PA (°) (68 per cent c.l.)	Π (per cent) (90 per cent c.l.)	PA (°) (90 per cent c.l.)
250–800	>60	150 ± 15	>33	150 ± 20
250–350	>65	145 ± 15	>35	145 ± 27
350–800	>52	160 ± 20	>20	160 ± 38

Table 2. Exposure times and measured magnitudes (1σ c.l.) for the host galaxy of GRB 061122. Galactic extinction along the line of sight has not been subtracted from the data.

Filter (System)	CFHT exp. Time (ks)	TNG exp. Time (ks)	Mag. Object 1	Mag. Object 2
$u^\star(AB)$	4.5		>24.5 (3σ)	>24.75 (3σ)
$g'(AB)$	1.5		>24.25 (3σ)	23.60 ± 0.12
$r'(AB)$	1.2	1.9	>24.0 (3σ)	23.15 ± 0.10
$i'(AB)$	1.1	1.8	>23.5 (3σ)	22.23 ± 0.08
$z'(AB)$	0.5	1.8	>23.0 (3σ)	21.74 ± 0.10
$Y(Vega)$	7.6		22.66 ± 0.25	20.64 ± 0.07
$J(Vega)$	7.6	2.6	22.31 ± 0.27	20.16 ± 0.06
$H(Vega)$	4.9		21.52 ± 0.33	19.65 ± 0.09
$K_s(Vega)$	5.7	5.3	20.63 ± 0.22	19.37 ± 0.10

3 HOST GALAXY IDENTIFICATION

3.1 TNG observations

The GRB 061122 field was observed with Dolores and NICS at the 3.5 m TNG in La Palma (Canary Islands, programme ID: AOT24/TAC_12) in queued observing mode. The Dolores data have been collected between 2011 August 1 and 5 in the r', i' and z' filters, while the NICS data have been obtained between 2011 August 12 and 15 in the J and K_s filters. During the Dolores observations the seeing was in the 0.5–1.0 arcsec interval, while during the NICS ones it ranged between 0.7 and 1.0 arcsec. Data for the TNG run (and the CHFT run) are reported in Table 2.

TNG data were reduced by means of a custom pipeline[1] implementing standard procedures. Data were bias/dark subtracted and flat-field correction was applied. Individual frames were shifted to a common reference and astrometry was derived on the final averaged images using the Two Micron All Sky Survey (2MASS) catalogue[2] as a reference. Aperture photometry was performed by means of the GAIA[3] tools and calibration was derived with suitable isolated non-saturated stars in the field using the photometry from the 2MASS catalogue in the near-infrared (NIR). For the optical data, we relied on the calibration carried out for the CFHT frames (see Section 3.2).

3.2 CFHT observations

The GRB 061122 field was observed with MegaCam and WIRCam at the 3.6 m CFHT in Mauna Kea (Hawaii, programme ID: 11BF020) in queued service observation mode. The MegaCam data were collected between September 6 and October 31 in the $u^\star$, g', r',i' and z' filters, while the WIRCam data were obtained between 2011 September 12 and October 12 in the Y, J, H and K_s filters. During the MegaCam observations the seeing was in the

[1] http://pypi.python.org/pypi/SRPAstro/
[2] http://www.ipac.caltech.edu/2mass/
[3] http://star-www.dur.ac.uk/~pdraper/gaia/gaia.html

0.8–1.2 arcsec interval, while during the WIRCam ones it ranged between 0.5 and 0.8 arcsec. Due to bad weather conditions, the MegaCam observation programme could not be completed resulting in the reduced exposure times reported in Table 2. In the same table, we report also the exposure for the NIR filters obtained with WIRCam.

As described in Götz et al. (2011), the CFHT data were reduced using the TERAPIX[4] pipeline. The latter retrieves pre-processed data from the CFHT data base, combines the mask and gain-maps of the individual images – obtaining the weight-maps, that are needed to perform image mosaicking – subtracts bias/dark images and produces flat-field images. Astrometry is then performed on individual images using a reference catalogue (USNO,[5] 2MASS) and a pattern matching algorithm. Then, overlapping detections are identified among the individual images and a global astrometric solution is computed. Photometry is then performed in a similar way, harmonizing the zero-points from the different pointings to account for different atmospheric extinctions and non-photometric observing conditions. Images are finally co-added, using the astrometric and photometric calibrations, and the weight-maps described above.

As for the TNG data, the GAIA package was used to perform the aperture photometry, and the final photometry, reported in Table 2, was derived by a weighted mean of the TNG and CFHT results when both are available.

3.3 GTC observations

We obtained observing time on the 10.4 m Gran Telescopio Canarias (GTC) in the Observatorio del Roque de los Muchachos (Canary Islands, Spain) to perform spectroscopy of the GRB host galaxy candidate. Our initial programme (ID 44-GTC17/11B) was accepted but could not be carried out, and our second programme (37-GTC8/12B) was successful. The observations were performed in queue mode on the night of 2012 August 20, under dark, clear conditions, with seeing approximately 1.0 arcsec.

GTC provided us with long-slit spectroscopic observations of the brightest candidate compatible with our early finding chart of the GRB field, obtained at TNG, where object 2 was the only detected source close to the XRT error box (see Section 3.4.1). We used the R300R grating ($R \approx 300$) and integrated for 4200 s on target. Standard calibration images and procedures were acquired and followed for wavelength calibration, and an approximate flux calibration was obtained using the spectrophotometric standard star GD190.

3.4 Photometry, spectroscopy and identification

3.4.1 Imaging

We have compared the most precise error boxes provided in the literature for GRB 061122, with our images. In particular, we used the *Swift*/XRT position, derived using 26 ks of data (Evans et al. 2010), provided by the Swift Science Data Centre (http://www.swift.ac.uk), corresponding to RA = $20^{\rm h}15^{\rm m}19\overset{\rm s}{.}87$ and Dec. = $+15^\circ31'01\overset{''}{.}8$ with an uncertainty of 1.4 arcsec, and the optical afterglow position published by Halpern & Armstrong (2006), obtained in the *R* band, and corresponding to RA = $20^{\rm h}15^{\rm m}19\overset{\rm s}{.}84$ and Dec. = $+15^\circ31'02\overset{''}{.}5$ with an uncertainty of 0.5 arcsec. As can be seen from our CFHT/WIRCam *J* band image (Fig. 4) there is

[4] http://terapix.iap.fr

[5] http://www.usno.navy.mil/USNO/astrometry/optical-IR-prod

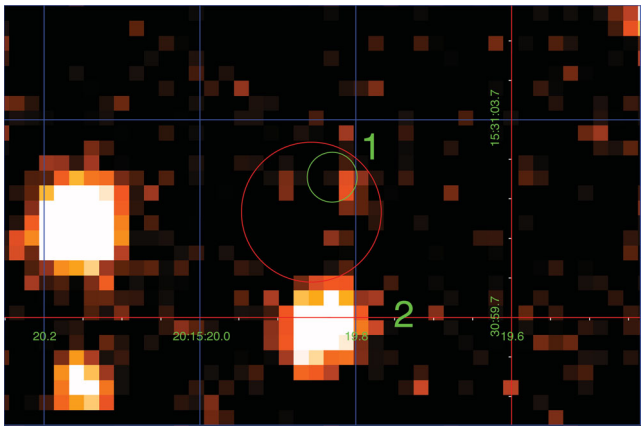

Figure 4. CFHT/WIRCam image of the GRB 061122 field obtained in the *J* filter. The red circle represents the *Swift*/XRT error box, while the smaller green circle represents the optical afterglow error box. Object 1 has been identified as the GRB host galaxy candidate.

only one bright object (labelled '2') that is marginally compatible with the XRT error box (drawn in red), while there is a faint object (labelled '1') that is compatible with both error boxes. We therefore identify the GRB 061122 host galaxy candidate with object 1. The latter is located at RA = $20^{\rm h}15^{\rm m}19\overset{\rm s}{.}81$ Dec. = $+15^\circ31'02\overset{''}{.}5$, and its measured magnitudes based on both data sets are reported in Table 2.

The source appears to be point-like in all frames where it is detected, although its faintness would have probably prevented any extension to be measured. It is detected only in the NIR, and this might be consistent with a high redshift source or a dusty sight line. However, the not negligible Galactic extinction along the line of sight, $E_{B-V} = 0.16$ (Schlafly & Finkbeiner 2011), makes optical detection, in particular in the bluer filters, even more demanding.

3.4.2 GTC spectroscopy

When this project started, prior to our CFHT/WIRCam observations, the object labelled as 'object 2' (AB(R) $\approx$ 23.2) in Fig. 4 was the only detected candidate which was barely compatible with the *Swift*/XRT observations. Hence, this is the object for which we performed the spectroscopic observations in order to measure its redshift. As mentioned above, we obtained time on the GTC telescope, and in Fig. 5 we show its spectrum, which does not feature prominent emission or absorption lines. Based on the presence of a possible 4000 Å break in the photometric data, and associated absorption lines, we adopt $z = 0.74$ as its redshift. The spectrum corresponds to that of a galaxy with an evolved stellar population, strengthening object 1 as being GRB 061122 host galaxy candidate, see below.

3.4.3 Spectral energy distribution modelling and distance determination

We have combined all our photometric observations from TNG and CFHT to produce a wide coverage spectral energy distribution (SED; *ugrizYJHK*) for the putative host of GRB 061122, see Table 2. We have corrected it for the observed galactic extinction ($E_{B-V} = 0.16$), and using these data and the photometric redshift code by Fernández-Soto, Lanzetta & Yahil (1999), we have estimated the redshift and basic properties of our host galaxy candidate, object 1.

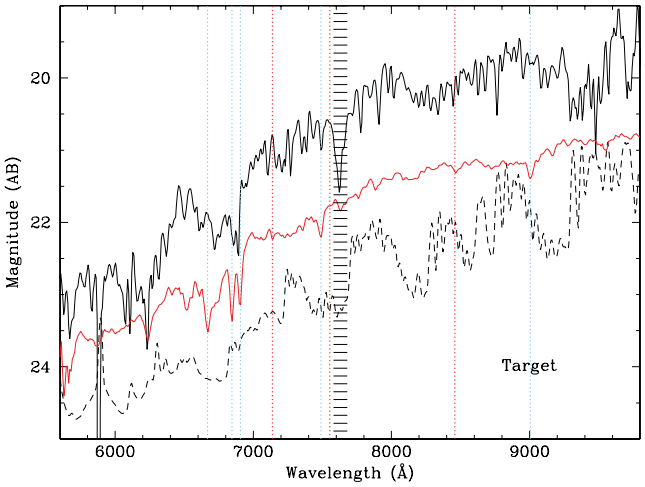

Figure 5. GTC spectrum of object 2 and its associated 1σ uncertainty are plotted as the continuous and dashed lines. The red line shows for comparison the template spectrum of an elliptical galaxy at redshift $z = 0.74$, with the vertical lines marking the position of the main emission and absorption features. The shaded area at $\lambda \approx 7600$ Å corresponds to the main atmospheric O_2 line.

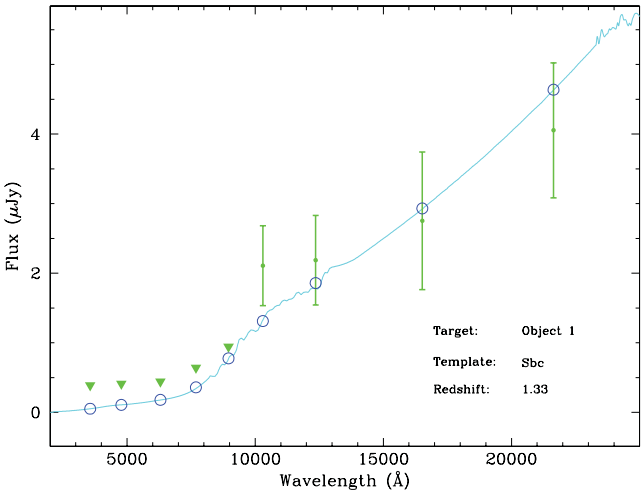

Figure 6. The plot shows our TNG and CFHT photometry for the host galaxy candidate as filled green circles with error bars, and as green arrows in the case of our 1σ upper limits. The best-fitting spectrum obtained for an Sb/c galaxy template at $z = 1.33$ is shown as a cyan line, and the expected photometry for such a model is indicated by the empty blue circles.

As shown in Table 2, object 1 is not detected in our *ugriz* images, and it is marginally seen in all the observed NIR bands (*YJHK*, in all of them between 3σ and 5σ significance). At face value this may point to a very high-redshift solution ($z \approx 7$), but such a galaxy would hardly be detectable in our data. Excluding this very high redshift solution, the best-fitting candidate is represented by a galaxy with an old stellar population template with redshift $z \in [0.38, 1.96]$.[6] However, old stellar population galaxies are less likely to host long GRBs, which are rather associated with galaxies with on-going star formation (see e.g. Savaglio, Glazebrook & Le Borgne 2009). Indeed, the second best-fitting candidate for our photometry is represented by an Sb/c template at a slightly higher redshift $z \in [0.57, 2.10]$. The best-fitting solution in this case, with $z = 1.33$, is shown in Fig. 6, and implies an isotropically equivalent emitted energy for the GRB of $E_{\rm iso} \sim 3 \times 10^{52}$ erg (1 keV–10 MeV).

4 LIV LIMITS

On general grounds one expects that the two fundamental theories of contemporary physics, the theory of General Relativity and the quantum theory in the form of the Standard Model of particle physics, can be unified at the Planck energy scale. This unification requires to quantize gravity, which leads to very fundamental difficulties: one of these is the possibility of LIV (e.g. Mattingly 2005; Jacobson, Liberati & Mattingly 2006; Liberati & Maccione 2009).

A possible experimental test of LIV is testing the helicity dependence of the propagation velocity of photons (see e.g. Laurent et al. 2011a, and references therein). The light dispersion relation is given in this case by

$$\omega^2 = k^2 \pm \frac{2\xi k^3}{M_{\rm Pl}} \equiv \omega_\pm^2, \qquad (2)$$

where $E = \hbar\omega$, $p = \hbar k$, $M_{\rm Pl}$ is the Planck mass, and the sign of the cubic term is determined by the chirality (or circular polarization) of the photons, which leads to a rotation of the polarization during the propagation of linearly polarized photons. This effect is known as vacuum birefringence.

Equation (2) can be approximated as follows:

$$\omega_\pm = |p|\sqrt{1 \pm \frac{2\xi k}{M_{\rm Pl}}} \approx |k| \left(1 \pm \frac{\xi k}{M_{\rm Pl}}\right), \qquad (3)$$

where ξ gives the order of magnitude of the effect. In other words, if a polarized signal is measured from a distant source, some quantum–gravity theories (e.g. Myers & Pospelov 2003) predict that the polarization plane should rotate by a quantity $\Delta\theta$ while the electromagnetic wave propagates through space, and this as a function of the energy of the photons. This is illustrated in equation (4), where d is the distance of the source:

$$\Delta\theta(p) = \frac{\omega_+(k) - \omega_-(k)}{2}\, d \approx \xi \frac{k^2 d}{2M_{\rm Pl}}. \qquad (4)$$

This implies that a polarized signal produced by a given source would vanish if observed on a broad energy band, since the differential rotation acting on the polarization angle as a function of energy would in the end add opposite oriented polarization vectors. But being this effect very tiny, since it is inversely proportional to the Planck mass ($M_{\rm Pl} \sim 2.4 \times 10^{18}$ GeV), the observed source needs to be at cosmological distances. So, the simple fact to detect the polarization signal from a distant source, can put a limit to such a possible violation. This experiment has been performed recently by Laurent et al. (2011a) and Toma et al. (2012) making use of GRBs. Indeed, since GRBs are cosmological, their polarization measurements are highly suited to measure and improve upon these limits. Laurent et al. (2011a), taking advantage from the polarization measurements obtained with IBIS on GRB 041219A in different energy bands (200–250 keV, 250–325 keV), and from the measure of distance of the source ($z > 0.02$ at 90 per cent c.l., equivalent to a luminosity distance 85 Mpc) were able to set the most stringent limit to date to a possible LIV effect: $\xi < 1.1 \times 10^{-14}$. We note that, although Toma et al. (2012) claim to have derived a more stringent limit ($\xi < 8 \times 10^{-16}$), their measure does not rely on a real measure of the distance of the GRBs they analyse, but they use a distance estimate based on an empirical spectral–luminosity relation

[6] All of the redshift intervals quoted are given at the 90 per cent c.l., and include a systematic error component calculated as in Fernandez-Soto et al. (2002).

(Yonetoku et al. 2010), whose selection effects, physical interpretation and absolute calibration are not yet completely understood.

By taking the 90 per cent c.l. lower limit on the distance of the host of GRB 061122 we derived through our multiband SED modelling, $z = 0.54$, corresponding to a luminosity distance of 3.309 Gpc ($\Omega_{\rm m} = 0.27$, $\Omega_{\lambda} = 0.73$ and $\rm H_0 = 71\ km\ s^{-1}\ Mpc^{-1}$), and if we set $\Delta\theta(k) = 80^{\circ}$ (see Table 1), we obtain

$$\xi < \frac{2M_{\rm Pl}\Delta\theta(k)}{(k_2^2 - k_1^2)\,d} \approx 3.4 \times 10^{-16}. \quad (5)$$

5 DISCUSSION AND CONCLUSIONS

We measured linear polarization in the gamma-ray energy band (250–800 keV) during the brightest part of the prompt emission of GRB 061122. We were able to put a lower limit on the polarization level of 33 per cent (90 per cent c.l.), and exclude an unpolarized signal at a probability level of 10^{-4}. This measure, follows some recent reports of detections of high (and variable) polarization levels in the prompt emission of a few other GRBs: 041219A by Götz et al. (2009), 100826A, 110301A and 110721A by Yonetoku et al. (2011, 2012). Although all these measures, taken individually, have not a very high significance ($\gtrsim 3\,\sigma$), they indicate that GRBs may indeed be emitters of polarized radiation. In addition, for the *INTEGRAL* bursts GRB 041219A and GRB 061122 there are independent and compatible measurements obtained by SPI and IBIS: for 061122, McGlynn et al. (2009), using SPI data, derived a measure (compatible with the one presented here) of $\Pi = 29^{-26}_{+25}$ per cent (1σ c.l., 100 keV–1 MeV) for the polarization level, but they could not constrain further this result due to lack of statistics; for bright GRB 041219A, McGlynn et al. (2007) and Götz et al. (2009) measured independently on a short interval during the GRB peak emission $\Pi = 68 \pm 29$ per cent (100 keV–1 MeV) and 65 ± 26 per cent (250 keV–800 keV), respectively. These are remarkably similar results, while the apparent discrepancy, pointed out by Yonetoku et al. (2011, 2012) on the measure of the polarization on a longer time interval, where Götz et al. (2009) put an upper limit on the polarization level of $\Pi < 4$ per cent, while McGlynn et al. (2007) detect a signal of 26 ± 20 per cent, can be easily reconciled by the fact that both measures provide errors at a 1σ c.l. In addition, the measurement on the longer time interval containing the peak is statistically largely dominated by the peak itself in the SPI data (the measured PA is actually the same for both intervals), while this is not the case in the IBIS data: due to the larger effective area with respect to SPI, IBIS records a much larger number of counts for a given source. But this has the drawback of losing some of the counts during transmission because of telemetry limitations at satellite level. The consequence for GRB 041219A was that in the IBIS data the bright peak (i.e. the short interval) had about the same number of counts than its wings, and hence the statistical coverage of the burst was more homogeneous over its different parts, allowing us, on one hand, to measure the variations of the PA, but implying, on the other hand, the net effect that the different portions of the GRB, with different PA, tend to wash out the polarization signal on a longer time interval.

As discussed in the works mentioned above, the measure of a high level of linear polarization, as well as its variability, point towards an interpretation where synchrotron radiation is emitted from shock accelerated electrons in a relativistic jet with a magnetic field transverse to the jet expansion. The coherence of the magnetic field geometry does not need to hold over the entire jet, but only over a small portion of it, since, due to relativistic effects, the observer can see only a region of the jet whose angular size is comparable to $1/\Gamma$, Γ being the Lorentz factor of the relativistic outflow. If the radiating electrons are accelerated in internal shocks (Rees & Mészáros 1994; Kobayashi, Piran & Sari 1997; Daigne & Mochkovitch 1998), then the Lorentz factor is necessarily varying in the outflow, which can explain the variability of the polarization from one pulse to the other (Granot 2003; Granot & Königl 2003; Nakar, Piran & Waxman 2003), as observed in GRB 041291A and GRB 100826A. This is not the only possible interpretation, and other models that predict locally coherent magnetic fields, like fragmented fireballs (shotguns, cannonballs, subjets) can produce highly polarized emission, with a variable polarization angle. In this frame, the fragments are responsible for the single pulses and have different Lorentz factors, opening angles and magnetic domains (e.g. Lazzati & Begelman 2009). In addition, different emission mechanisms cannot be completely excluded at this time, implying random magnetic fields and peculiar observing conditions, like e.g. inverse Compton scattering (Lazzati et al. 2004). Only when more data with a higher accuracy become available, some model will be preferred on the basis of statistical arguments. On the other hand, to be able to quantitatively compare the data with the theory, more accurate models are also needed.

Thanks to our late time imaging of the field of GRB 061122 obtained with the TNG and the CFHT, we were able to identify the host galaxy of GRB 061122, and to constrain through multiband optical and NIR SED modelling, its type, and its distance to the redshift interval [0.57, 2.10]. The latter together with the polarization measure obtained with IBIS, allowed us to derive the deepest and most reliable limit available to date ($\xi < 3.4 \times 10^{-16}$) on the possibility of LIV, measured through the vacuum birefringence effect on a cosmological source.

ACKNOWLEDGEMENTS

Based on observations with *INTEGRAL*, an ESA project with instruments and science data centre funded by ESA member states (especially the PI countries: Denmark, France, Germany, Italy, Switzerland, Spain), Czech Republic and Poland, and with the participation of Russia and the USA, on observations obtained with WIRCam, a joint project of CFHT, Taiwan, Korea, Canada, France, and with MegaCam, a joint project of CFHT and CEA/Irfu, at the Canada–France–Hawaii Telescope (CFHT) which is operated by the National Research Council (NRC) of Canada, the Institute National des Sciences de l'Univers of the Centre National de la Recherche Scientifique of France, and the University of Hawaii, and on observations made with the Gran Telescopio Canarias (GTC), installed in the Spanish Observatorio del Roque de los Muchachos of the Instituto de Astrofísica de Canarias, on the island of La Palma. ISGRI has been realized and maintained in flight by CEA-Saclay/Irfu with the support of CNES. The authors are grateful to the TERAPIX team (http://terapix.iap.fr/) for providing the CHFT data reduction. AFS acknowledges support from the Spanish MICYNN projects AYA2010-22111-C03-02 and Consolider-Ingenio 2007-32022, and from the Generalitat Valenciana project Prometeo 2008/132.

REFERENCES

Amati L., 2007, MNRAS, 372, 233
Arnaud K. A., 1996, in Jacoby G. H., Barnes J., eds, ASP Conf. Ser. Vol. 101, Astronomical Data Analysis Software and Systems V. Astron. Soc. Pac., San Francisco, p. 17
Band D. et al., 1993, ApJ, 413, 281
Bloom J. S., Frail D. A., Kulkarni S. R., 2003, ApJ, 594, 674

Bošnjak Ž., Götz D., Bouchet L., Schanne S., Cordier B., 2013, submitted
Daigne F., Mochkovitch R., 1998, MNRAS, 296, 275
Di Cocco G. et al., 2003, A&A, 411, L189
Evans P. A. et al., 2010, A&A, 519, A102
Fan Y.-Z., Wei D.-M., Xu D., 2007, MNRAS, 376, 1857
Fernández-Soto A., Lanzetta K. M., Yahil A., 1999, ApJ, 513, 34
Fernández-Soto A., Lanzetta K.M, Chen H.-W., Levine B., Yahata N., 2002, MNRAS, 330, 889
Forot M., Laurent P., Grenier I. A., Gouiffès C., Lebrun F., 2008, ApJ, 688, L29
Frail D. A. et al., 2001, ApJ, 562, L55
Gambini R., Pullin J., 1999, Phys. Rev. D, 59, 124021
Gehrels N., Ramirez-Ruiz E., Fox D. B., 2009, ARA&A, 47, 567
Ghirlanda G., Nava L., Ghisellini G., Celotti A., Burlon D., Covino S., Melandri A., 2012, MNRAS, 420, 483
Golenetskii S., Aptekar R., Mazets E., Pal'shin V., Frederiks D., Cline T., 2006, GCN Circ., 5841
Götz D., Laurent P., Lebrun F., Daigne F., Bošnjak Ž., 2009, ApJ, 695, L208
Götz D., Covino S., Hascoët R., Fernandez-Soto A., Daigne F., Mochkovitch R., Esposito P., 2011, MNRAS, 413, 2173
Granot J., 2003, ApJ, 596, L17
Granot J., Königl A., 2003, ApJ, 594, L83
Halpern J., Armstrong E., 2006, GCN Circ., 5849
Jacobson T., Liberati S., Mattingly D., 2006, Ann. Phys., 321, 150
Kalemci E., Boggs S. E., Kouveliotou C., Finger M., Baring M. G., 2007, ApJS, 169, 75
Kobayashi S., Piran T., Sari R., 1997, ApJ, 490, 92
Laurent P., Götz D., Binétruy P., Covino S., Fernandez-Soto A., 2011a, Phys. Rev. D, 83, 121301
Laurent P., Rodriguez J., Wilms J., Cadolle Bel M., Pottschmidt K., Grinberg V., 2011b, Sci, 332, 438
Lazzati D., Begelman M. C., 2009, ApJ, 700, L141
Lazzati D., Rossi E., Ghisellini G., Rees M. J., 2004, MNRAS, 347, L1
Lebrun F. et al., 2003, A&A, 411, L141
Liberati S., Maccione L., 2009, Annu. Rev. Nucl. Part. Sci., 59, 245
Lyutikov M., 2006, New J. Phys., 8, 199
Mattingly D., 2005, Living Rev. Relativ., 8, 5
McGlynn S. et al., 2007, A&A, 466, 895
McGlynn S. et al., 2009, A&A, 499, 465
Mereghetti S., Götz D., Borkowski J., Walter R., Pedersen H., 2003, A&A, 411, L291
Mereghetti S., Paizis A., Götz D., Petry D., Mowlavi N., Beck M., Borkowski J., 2006, GCN Circ., 5834
Myers R. C., Pospelov M., 2003, Phys. Rev. Lett., 90, 211601
Nakar E., Piran T., Waxman E., 2003, J. Cosmol. Astropart. Phys., 10, 005
Rees M. J., Mészáros P., 1994, ApJ, 430, L93
Rhoads J. E., 1997, ApJ, 487, L1
Savaglio S., Glazebrook K., Le Borgne D., 2009, ApJ, 691, 182
Schlafly E. F., Finkbeiner D. P., 2011, ApJ, 737, 103
Spruit H. C., Daigne F., Drenkhahn G., 2001, A&A, 369, 694
Toma K. et al., 2012, Phys. Rev. D, 109, 24, 241104
Ubertini P. et al., 2003, A&A, 411, L131
Vianello G., Götz D., Mereghetti S., 2009, A&A, 495, 1005
Winkler C. et al., 2003, A&A, 411, L1
Yonetoku D. et al., 2010, PASJ, 62, 1495
Yonetoku D. et al., 2011, ApJ, 743, L30
Yonetoku D. et al., 2012, ApJ, 758, L1
Zhang B.-B. et al., 2011, ApJ, 730, 141

This paper has been typeset from a TEX/LATEX file prepared by the author.